Spatial Data Focusing using Time and IQ Resources for Wireless Geocasting

Guylian Molineaux
Wireless Communications Group
Université Libre de Bruxelles
1050 Brussels, Belgium;
Laboratory of Electronics and Electromagnetics
Sorbonne Université
F-75005 Paris, France
gmolinea@ulb.ac.be

Sidney Golstein
Laboratory of Electronics and Electromagnetics
Sorbonne Université
F-75005 Paris, France;
Wireless Communications Group
Université Libre de Bruxelles
1050 Brussels, Belgium

Michael Odhiambo
Laboratory of Electronics and Electromagnetics
Sorbonne Université
F-75005 Paris, France;
Wireless Communications Group
Université Libre de Bruxelles
1050 Brussels, Belgium

François Horlin
Wireless Communications Group
Université Libre de Bruxelles
1050 Brussels, Belgium

Philippe De Doncker
Wireless Communications Group
Université Libre de Bruxelles
1050 Brussels, Belgium

Julien Sarrazin
Laboratory of Electronics and Electromagnetics
Sorbonne Université
F-75005 Paris, France

***Abstract*—Spatial Data Focusing (SDF) is introduced as a novel technique that allows wireless broadcasting of information towards specific spatial locations only. It is shown that this approach allows one to target geographic areas more accurately than traditional power focusing methods, using limited equipment at the transmitter. This paper describes the SDF system model for linear arrays, based on simple modulation techniques and transmitter architectures, both in pure line-of-sight and multi-path environments. In particular, the robustness of the scheme is proven for over-the-ground propagation environments. Theoretic results are illustrated by simulations, confirming the increased spatial selectivity of SDF and showing the influence of various design parameters of the scheme on the resulting beam.**

***Index Terms*—Geocasting, Spatial Data Focusing, Wireless Communications**

I. Introduction

Geocasting refers to the transmission of information towards specific geographic areas. This is useful in a wide range of applications, like tourism, traffic, management, marketing, etc., that use information related or contextualized to the user's location. Providing location aware information often requires that applications have knowledge of the user's position, which may lead to privacy issues. Geocasting, on the other hand, broadcasts data not to a user but to a geographical area, such that all users inside a predefined zone have access to the data without necessarily needing to share their location.

Geocasting can be performed based on geographic routing algorithms, like in [1] and [2], that tackle the issue as location-based multicasting. These techniques, however, make use of multihopping methods that require nodes being equipped with localization mechanisms to detect their own position and compare it to the location address indicated in packets. To remove the requirement of cooperative nodes that perform self-localization, information can be routed towards selected base stations that forward the data to all nodes within their range. In this case, the geocasting accuracy is fully determined by the base station coverage. To increase this accuracy, base stations need to exhibit spatial focusing capabilities.

A traditional approach to spatial focusing is beamforming, which makes use of antenna arrays transmitting complex weighted signals, causing constructive interference in some directions and destructive interference elsewhere [3]. In doing so, spatial selectivity is obtained by focusing power in the spatial domain. Beamforming, however, suffers from the physical limitation that the beamwidth is related to the electrical size of the array and achieving narrow beams hence requires large arrays. In order to overcome this limitation, we suggest in this paper a technique that allows one to target an area not by focusing power, but by performing Spatial Data Focusing (SDF). Unlike beamforming, SDF transmits uncorrelated signals over each antenna in an array, that represent the dimensions of a multi-dimensional orthogonal symbol space. The idea is that, depending on the receiver's position, the orthogonality of the transmitted signals, and equivalently, the orthogonality of the symbol space, can be either preserved or lost. By ensuring that orthogonality is preserved only in the intended communication direction, symbols will be decoded incorrectly elsewhere and hence

This work was supported by the ANR GEOHYPE project, grant ANR-16-CE25-0003 of the French Agence Nationale de la Recherche, as well as the FNRS/FRIA and EOS MUSE-WINET programs, and carried out in the framework of COST Action CA15104 IRACON.

SDF achieves data focusing by ensuring a low bit error rate (BER) only within a given angular range and a high BER elsewhere.

To some extent this approach is similar to Directional Modulation (DM) techniques, that define specific modulation schemes to create decoding ambiguities in certain directions. DM approaches in [4] and [5] realize this by using arrays of reconfigurable antennas, whose near-field radiation pattern can be modified such that the far-field radiation behaviour of the array has the phase and amplitude characteristics of the desired symbol in the focus direction only. However, due to the limited set of states of the reconfigurable antennas, these schemes are restricted by limited flexibility and complex synthesis processes. The second type of DM transmitters, as presented in [6]–[9], act as an extension to beamforming, by calculating for each symbol a unique weighing vector for the array, such that symbols can only be unambiguously decoded in the beamforming main lobe direction. While being more synthesis friendly, these approaches, however, do not release the constraints of beamforming and serve mostly as a means of securing wireless links against eavesdropping in array sidelobe directions, providing only limited improvements in terms of spatial selectivity. SDF, on the other hand, expands the concept of DM from security to spatial focusing. By releasing the constraint on the array radiation pattern, greater spatial selectivity than beamforming or DM is obtained, expressed in terms of the angular range around the transmitter for which the BER is below a given threshold.

Preliminary work [10] has introduced the idea of using time resources to achieve SDF. However, additional degrees of freedom, leading to increased spatial selectivity, can be introduced by using quadrature amplitude modulated time signals, as discussed in this paper.

Section II describes the free space system model used for SDF, and compares the focusing performance to beamforming. Section III extends this model to multipath environments and specifically proves the robustness of SDF in an over-the-ground propagation environment. Finally, conclusions are drawn in Section IV.

II. Free Space Spatial Data Focusing Model

A. System model and received symbols

Fig. 1 shows the system model that is used for SDF in free space. At its input, the transmitter maps a bitstream onto a $2N$-dimensional orthogonal symbol space, using a rectangular mapping scheme. This results in N quadrature amplitude modulated symbol streams $S_i[n] = I_i[n] - jQ_i[n]$, $i \in \{0, 1, \ldots, N-1\}$, each containing an in-phase (I) and quadrature (Q) component, $I_i[n]$ and $Q_i[n]$ respectively. Each sequence $S_i[n]$ is shaped with a corresponding root-raised cosine filter $g_i(t) = g(t - i\frac{T_d}{N})$, where T_d is the symbol period, $g(t)$ a root-raised cosine filter with bandwidth $B = N/T_d$, and

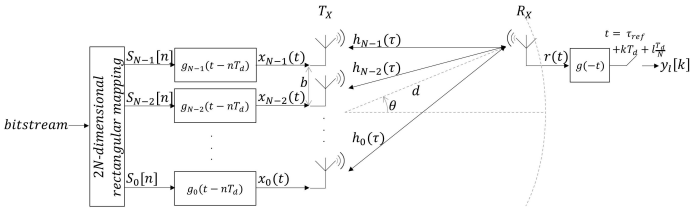

Fig. 1. SDF free space system model

$\langle g_i(t), g_j(t) \rangle = 0$, $\forall i, j \in \{0, 1, \ldots, N-1 | i \neq j\}$. In doing so, the N resulting signals

$$x_i(t) = \sum_{n=-\infty}^{+\infty} S_i[n] g_i(t - nT_d) \tag{1}$$

become orthogonal in the time domain and can be transmitted over their corresponding antennas of a linear N-element array at the base station.

Each signal $x_i(t)$ is transmitted by a different antenna and hence propagates through a different channel. Assuming a perfect line-of-sight (LOS) environment, the baseband channel impulse response $h_i(\tau)$ of the i-th channel is given by

$$h_i(\tau) = a_i \delta(\tau - \tau_i) e^{j\phi_i} e^{-j2\pi f_c \tau_i} \tag{2}$$

where τ is the delay, a_i is the channel attenuation, τ_i is the propagation delay of the channel, ϕ_i the phase shift introduced by the channel, and f_c the carrier frequency. The total received baseband signal $r(t)$ can therefore be expressed as

$$r(t) = \sum_{i=0}^{N-1} x_i(t) * h_i(\tau) \tag{3a}$$

$$= \sum_{i=0}^{N-1} a_i x_i(t - \tau_i) e^{j\phi_i} e^{-j2\pi f_c \tau_i} \tag{3b}$$

At the receiver, who is cooperative in the sense that it is aware of the specific scheme that is used, one of the channels $h_i(\tau)$ (e.g. the first antenna's channel) is selected as the reference for the channel estimation process. Equalization of all channels is performed using the same unique estimation of the reference channel. To introduce this in the model, the propagation delay of the i-th channel is written as $\tau_i = \tau_{ref} + \Delta\tau_i$, where τ_{ref} is the propagation delay of the designated reference channel and $\Delta\tau_i$ is the relative delay difference of the i-th channel with respect to this reference delay. Similarly, a_i and ϕ_i could be expressed relative to the reference channel. However, if the antenna spacing in the array is smaller than the channel coherence distance, as is the case in this free space scenario, it can be assumed that these parameters are equal for all channels, i.e. $a_i \approx a$ and $\phi_i \approx \phi$, $\forall i$ in (2).

The receiver will then project the received signal on each dimension of the symbol space. By convolving $r(t)$ with the matched filter $g(-t)$ of the root-raised cosine pulse

used at the transmitter and subsequent sampling, assuming perfect synchronization with the reference channel, i.e. at $t = \tau_{ref} + kT_d + l\frac{T_d}{N}$, $k \in \mathbb{Z}$, $l \in \{0, 1, \ldots, N-1\}$, the l-th pair of IQ components of the k-th received symbol can be extracted, yielding

$$y_l[k] = aS_l[k]e^{j\phi}e^{-j2\pi f_c \tau_{ref}}e^{-j2\pi f_c \Delta\tau_l} \tag{4}$$

where a narrowband scenario is assumed, such that $\Delta\tau_l \ll \frac{T_d}{N}$, and the sampling offsets due to the delays $\Delta\tau_l$ can be neglected.

From (4), the functionality of SDF becomes clear. By equalizing all channels using the estimation of the reference channel, the influence of a, ϕ, and τ_{ref}, who are present for all channels, on the received symbols is neutralized. However, the influence of the relative delay differences $\Delta\tau_l$ remains. A simple Zero Forcing (ZF) equalization leads to

$$y_l[k] = S_l[k]e^{-j2\pi f_c \Delta\tau_l} \tag{5}$$

where the corresponding I and Q components can be expressed respectively as

$$y_l^I[k] = \cos(2\pi f_c \Delta\tau_l) I_l[k] - \sin(2\pi f_c \Delta\tau_l) Q_l[k] \tag{6a}$$

$$y_l^Q[k] = \cos(2\pi f_c \Delta\tau_l) Q_l[k] + \sin(2\pi f_c \Delta\tau_l) I_l[k] \tag{6b}$$

Under the paraxial approximation, i.e. $b \ll d$ (b being the antenna spacing in the array and d the distance between the receiver and the array center), for receivers located in the broadside direction of the array, all channels will have similar propagation path lengths, implying that $\Delta\tau_l \approx 0$, $\forall l$. As a consequence, the sine terms in (6a) and (6b) become negligible and the cosines are approximately one. The l-th in-phase (resp. quadrature) component of the transmitted symbol is thus correctly projected on the in-phase (resp. quadrature) dimension at the receiver. Orthogonality between the symbol's dimensions is preserved and the symbol constellation is not distorted. On the other hand, once receivers move away from the broadside direction, path length differences are introduced between the different channels, leading to an increase (in absolute value) of the delay differences $\Delta\tau_l$. This will distort the constellation, according to (6a) and (6b), eventually leading to decoding errors, making communication impossible in these directions. SDF consequently achieves data focusing by ensuring a low BER only within a given angular range around the base station and a high BER elsewhere. This region of low BER is unique, i.e. no sidelobes are present, on the condition that $b < \lambda_c$ (λ_c being the carrier wavelength). Note that the focus direction can easily be steered by introducing at the transmitter, for each channel i, an additional phase shift ϕ_i^{steer} to the transmitted signal $x_i(t)$, such that $\phi_i^{steer} - 2\pi f_c \Delta\tau_i = 0$ in the intended communication direction.

B. Evaluation of the beamwidth

For SDF, the beamwidth is defined as the region of receiver positions for which the BER is below a given threshold. The receiver position is expressed as a function of the polar coordinates (d, θ), where d represents the distance from the receiver to the array center and θ the angle with respect to the broadside direction of the array, as in Fig. 1. Again under paraxial approximation, the relative delay difference between each pair of neighbouring antennas in the array is $\Delta\tau = \frac{b}{c}\sin\theta$, where c is the speed of light. Hence it suffices to represent the receiver's position by the angle θ and express the beamwidth as the angular range where the BER is below the chosen threshold. To evaluate the beamwidth, an arbitrary threshold of uncoded $BER = 10^{-3}$ is chosen.

Unless specified otherwise, simulations are performed using the following parameters. A stream of 10^5 bits is generated and mapped onto $2N$-dimensional symbols containing $k = 2Nk_{dim}$ bits, where the parameter representing the number of bits encoded on a single dimension is set at $k_{dim} = 2$. The number of antennas is $N = 2$, with a spacing $b = 0.5\lambda_c$.[1] Equalization is performed using the estimation of the channel of the first antenna in the array. Finally, the carrier frequency is chosen as $f_c = 2.45$ GHz and the bandwidth as $B = 20$ MHz. The receiver moves on a circle around the array center at a distance $d = 1000\lambda_c$. Simulations are performed at a signal-to-noise ratio (SNR) of 25 dB.

For each configuration, the beamwidths obtained with SDF are compared to the ones obtained using beamforming (BF). The beamforming curves are obtained by uniformly feeding each antenna in the linear array with the same signal $x(t)/\sqrt{N}$. As a result, the transmitted power will vary according to the array factor, and so will the BER. The factor $1/\sqrt{N}$ is introduced to obtain the same transmitted power (and thus BER) in broadside for the SDF and beamforming arrays, such that a fair comparison can be made.

Fig. 2 and 3 illustrate how the beamwidth can be modified by altering the physical array dimensions. They show, respectively, the effect of varying the number of antennas N and the antenna spacing b, while keeping the other parameters constant. Increasing any of these parameters results in a narrower beam. This is easily understood since the delay differences between channels are of course proportional to the physical dimensions of the array, and hence, adding antennas or separating the antennas further results in greater delay differences between antennas and thus in larger symbol distortion for the same receiver positions. Note that, when the bandwidth $B = N/T_d$ is constant, increasing the number of antennas results in a lower symbol rate, however the number of bits coded per symbol increases, such that the bit rate is independent from the number of antennas. Clearly, SDF's angular focusing accuracy considerably exceeds the one attained by beamforming. Moreover, note that in Fig. 3, at $b = 0.25\lambda_c$, beamforming's power focusing is insufficient to create any region of high BER and additionally, for

[1]Note that the parameters N, b, and k_{dim} are varied in respectively Fig. 2, 3, and 4, but are fixed for all other simulations.

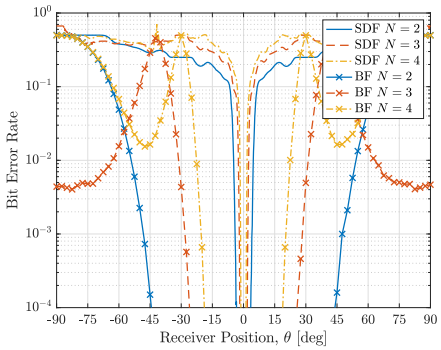

Fig. 2. Spatial BER distribution for different numbers of antennas ($f_c = 2.45$ GHz, $B = 20$ MHz, $b = 0.5\lambda_c$, $k_{dim} = 2$, $SNR = 25$ dB)

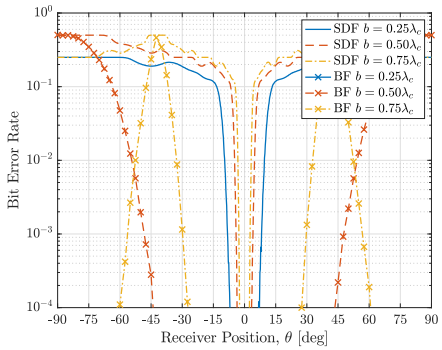

Fig. 3. Spatial BER distribution for different antenna spacings ($f_c = 2.45$ GHz, $B = 20$ MHz, $N = 2$, $k_{dim} = 2$, $SNR = 25$ dB)

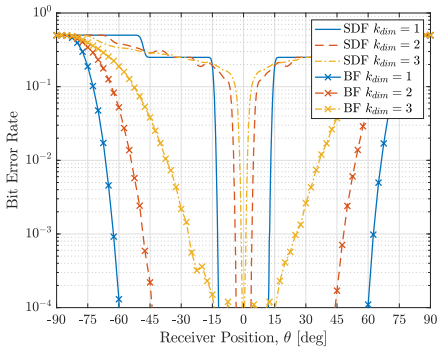

Fig. 4. Spatial BER distribution for different constellation sizes ($f_c = 2.45$ GHz, $B = 20$ MHz, $N = 2$, $b = 0.5\lambda_c$, $SNR = 25$ dB)

$b = 0.75\lambda_c$, beamforming's beam is narrowed, however at the cost of sidelobes appearing in the array radiation pattern (and thus also in the BER profile).

Fig. 4 shows the effect of varying the constellation size of the transmitted symbols, by varying the number of bits coded per dimension k_{dim}. Larger constellations result in narrower beams, since neighbouring symbols are closer and thus decoding errors are introduced for smaller distortions, i.e. for smaller delay differences. The increase in spatial selectivity of SDF with respect to beamforming is again clearly visible.

Finally, Fig. 5 compares the beamwidths of SDF and beamforming, as a function of the number of antennas in the array. Again it is obvious that SDF outperforms beamforming, achieving with only 2 antennas the same beamwidth for which beamforming needs 7 antennas and additionally increased noise power and antenna spacing. If one keeps the antenna spacing and SNR equal to the SDF case, no less than 19 antennas (not shown in the figure) are needed for beamforming to achieve the same beamwidth that SDF achieves with only 2 antennas.

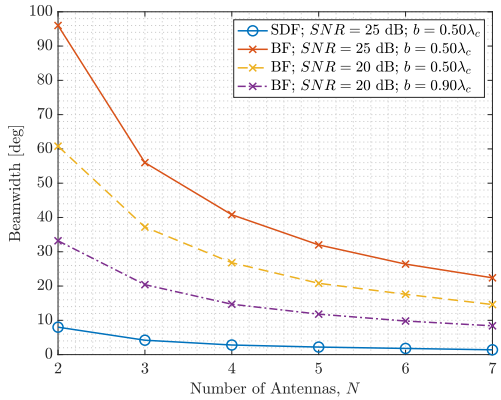

Fig. 5. Beamwidth comparison (at uncoded BER of 10^{-3}) as a function of the number of antennas N ($f_c = 2.45$ GHz, $B = 20$ MHz)

III. Effect of Multipath Environments

Multipath components (MPC) alter the amplitude and, more importantly for SDF, the phase of the channels over which the symbol components are transmitted. The presence of multipaths hence influences the potential loss of orthogonality between the symbol dimensions and should thus be taken into account when using SDF in non free space environments.

A. Channel model and received symbols

Adding a single multipath to the baseband channel impulse response (2) yields

$$h_i(\tau) = h_i^{LOS}(\tau) + h_i^{MPC}(\tau) \tag{7a}$$

$$= a_i^{LOS}\delta(\tau - \tau_i^{LOS})e^{j\phi_i^{LOS}}e^{-j2\pi f_c \tau_i^{LOS}} + a_i^{MPC}\delta(\tau - \tau_i^{MPC})e^{j\phi_i^{MPC}}e^{-j2\pi f_c \tau_i^{MPC}} \tag{7b}$$

where same notations as in Section II are used. Additionally, the superscripts ^{LOS} and ^{MPC} are used to distinguish between the LOS and MPC contributions to the impulse response respectively. It is again assumed that the antenna spacing in the array is smaller than the channel coherence distance and hence $a_i^{LOS} \approx a^{LOS}$, $\phi_i^{LOS} \approx \phi^{LOS}$, $a_i^{MPC} \approx a^{MPC}$, and $\phi_i^{MPC} \approx \phi^{MPC}$.

The l-th pair of IQ symbol dimensions of the k-th received symbol is now given by

$$y_l[k] = a^{LOS}S_l[k]e^{j\phi^{LOS}}e^{-j2\pi f_c \tau_l^{LOS}} + a^{MPC}S_l[k]e^{j\phi^{MPC}}e^{-j2\pi f_c \tau_l^{MPC}} \tag{8}$$

where a narrowband scenario is assumed, such that the MPC and LOS components are summed up in the same tap.

Like previously, the received symbol components from each channel are equalized using the estimation of the reference channel. All channel delays should thus again be expressed relative to the reference channel. Similarly to the pure LOS analysis, the LOS delay τ_l^{LOS} of the l-th channel is expressed with respect to the LOS delay τ_{ref}^{LOS} of the reference channel. Next, the delays τ_l^{MPC} of the multipath from each channel

are expressed, in a similar way, relative to the delay τ_{ref}^{MPC} of the multipath in the reference channel. Finally, the delay τ_{ref}^{MPC} of the multipath in the reference channel is expressed relative to the LOS propagation delay τ_{ref}^{LOS} of the reference channel, such that this delay is used as absolute reference. This is summarized in the equations below

$$\tau_l^{LOS} = \tau_{ref}^{LOS} + \Delta\tau_l^{LOS} \tag{9a}$$
$$\tau_l^{MPC} = \tau_{ref}^{MPC} + \Delta\tau_l^{MPC} \tag{9b}$$
$$= \tau_{ref}^{LOS} + \Delta\tau_{ref}^{MPC} + \Delta\tau_l^{MPC} \tag{9c}$$

Introducing these notations in (8) yields

$$y_l[k] = a^{LOS} S_l[k] e^{j\phi^{LOS}} e^{-j2\pi f_c \tau_{ref}^{LOS}} \Big[e^{-j2\pi f_c \Delta\tau_l^{LOS}} + \frac{a^{MPC}}{a^{LOS}} e^{-j2\pi f_c \Delta\tau_{ref}^{MPC}} e^{-j2\pi f_c \Delta\tau_l^{MPC}} \Big] \tag{10}$$

assuming that, since the LOS and MPC rays travel through the same medium, $\phi^{MPC} \approx \phi^{LOS}$. Note that, by linearity of the summation operator, this model can easily be expanded to include an arbitrary number of multipaths.

B. Over-the-ground Propagation Scenario

As a first multipath scenario analysis, an over-the-ground propagation environment is considered.

1) Setup Geometry: A linear array, oriented along the y-axis (according to Fig. 6), with the center at the origin, is considered at the transmitter. All antennas in the array are at equal height h_{Tx} above an infinite flat ground plane, parallel to the array and the xy-plane. Similar to the pure LOS case, the receiver position in the xy-plane is expressed using the polar coordinates d and θ, d being the radial distance, measured along the ground plane this time, from the array center to the receiver and θ the angle with respect to the broadside direction of the array. The receiver is located at height h_{Rx} above the ground.

Fig. 6 shows the geometry inside the plane of incidence of the i-th channel, allowing to define the propagation path lengths r_i^{LOS} and r_i^{MPC} of respectively the LOS ray and ground reflected ray of the i-th channel as

$$r_i^{LOS} = \sqrt{(h_{Tx} - h_{Rx})^2 + d_i^2} \tag{11a}$$
$$r_i^{MPC} = \sqrt{(h_{Tx} + h_{Rx})^2 + d_i^2} \tag{11b}$$
$$= \sqrt{r_i^{LOS^2} + 4h_{Tx}h_{Rx}} \tag{11c}$$
$$\approx r_i^{LOS}\left(1 + \frac{1}{2}\frac{4h_{Tx}h_{Rx}}{r_i^{LOS^2}}\right) \tag{11d}$$

where d_i is the distance, measured along the ground, between the i-th transmitting antenna and the receiver, and the approximation holds when $r_i^{LOS} \gg h_{Tx}, h_{Rx}$.

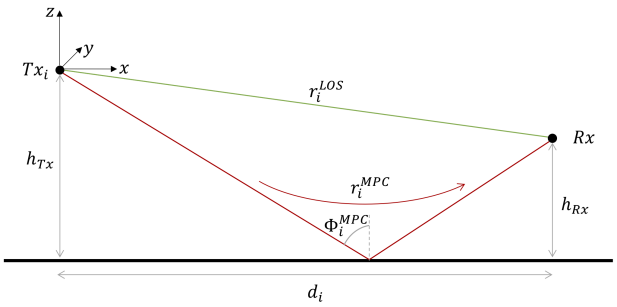

Fig. 6. Plane of incidence of the i-th channel

2) Received symbols: In (10), the parameters a^{LOS}, ϕ^{LOS}, and τ_{ref}^{LOS} are present for all channels and are not part of the complex sum, hence their influence will be removed after equalization. Their exact values are thus irrelevant in this analysis.

Applying (11d) to the l-th channel and the reference channel, and taking the difference, yields the relative path length difference Δr_l^{MPC} between the path lengths of the ground reflected ray of the l-th channel and the reference channel

$$\Delta r_l^{MPC} = r_l^{MPC} - r_{ref}^{MPC} \tag{12a}$$
$$\approx r_l^{LOS} - r_{ref}^{LOS} + \frac{2h_{Tx}h_{Rx}}{r_l^{LOS}} - \frac{2h_{Tx}h_{Rx}}{r_{ref}^{LOS}} \tag{12b}$$
$$= \Delta r_l^{LOS}\left[1 - \frac{2h_{Tx}h_{Rx}}{r_l^{LOS} r_{ref}^{LOS}}\right] \tag{12c}$$

The ratio $\frac{2h_{Tx}h_{Rx}}{r_l^{LOS} r_{ref}^{LOS}}$ quickly converges to zero when r_{ref}^{LOS} and r_l^{LOS} increase with respect to h_{Tx} and h_{Rx}. Under this assumption, the path length differences Δr_l^{LOS} and Δr_l^{MPC} (and hence also the delay differences $\Delta\tau_l^{LOS}$ and $\Delta\tau_l^{MPC}$) between respectively the LOS rays and the ground reflected rays of the l-th channel and reference channel, are approximately equal

$$\Delta r_l^{MPC} \approx \Delta r_l^{LOS} \tag{13a}$$
$$\Delta\tau_l^{MPC} \approx \Delta\tau_l^{LOS} \tag{13b}$$

Using this information in (10) yields

$$y_l[k] \approx a^{LOS} S_l[k] e^{j\phi^{LOS}} e^{-j2\pi f_c \tau_{ref}^{LOS}} \Big[1 + \frac{a^{MPC}}{a^{LOS}} e^{-j2\pi f_c \Delta\tau_{ref}^{MPC}}\Big] e^{-j2\pi f_c \Delta\tau_l^{LOS}} \tag{14a}$$
$$= y_l^{ref}[k] e^{-j2\pi f_c \Delta\tau_l^{LOS}} \tag{14b}$$

where $y_l^{ref}[k]$ represents the received l-th pair of IQ components with only the influence of the reference channel taken into account. Thanks to the fact that $\Delta\tau_l^{MPC} \approx \Delta\tau_l^{LOS}$, the influence of the reference channel and the l-th channel can be separated. After ZF equalization with respect to the reference channel, all effects of the reference channel disappear, yielding

$$y_l[k] \approx S_l[k] e^{-j2\pi f_c \Delta\tau_l^{LOS}} \tag{15}$$

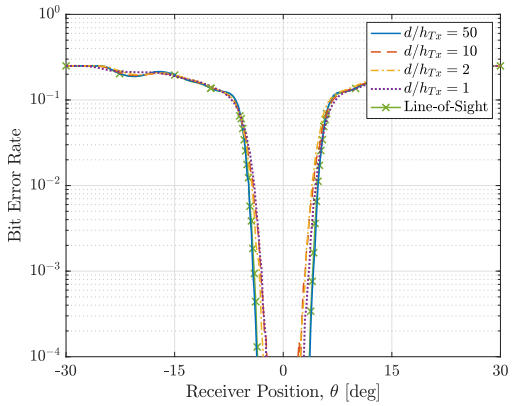

Fig. 7. Spatial BER distribution of SDF in an over-the-ground propagation environment for different distances between array and receiver ($f_c = 2.45$ GHz, $B = 20$ MHz, $N = 2$, $b = 0.5\lambda_c$, $k_{dim} = 2$, $SNR = 25$ dB)

This behaviour is in fact identical to the behaviour (5) that was obtained in Section II for a pure LOS scenario. As a result, the exact value of the remaining MPC parameters, a^{MPC} and $\Delta\tau_{ref}^{MPC}$, is of no importance and will not be derived. We can thus conclude that the presence of reflections off a ground plane has no significant influence on the performance of SDF with linear arrays, assuming that transmitter and receiver are far enough apart.

3) Evaluation of the beamwidth: In order to verify the conclusions drawn in the previous section, the simulations from Section II are repeated using the over-the-ground model. The same simulation parameters are used. For simplicity, the heights of transmitter and receiver are chosen to be equal at $h_{Tx} = h_{Rx} = 20\lambda_c$. The relative permittivity of the ground is chosen at $\varepsilon_r = 4.5$ and all antennas are assumed to have the same polarization, parallel to the planes of incidence. Of course, simulations were carried out without applying the approximation $r_i^{LOS} \gg h_{Tx}, h_{Rx}$.

Fig. 7 shows the spatial BER distribution for SDF in over-the-ground propagation scenarios, as a function of the array azimuth angle θ, for different distances between the array and the receiver (expressed as the ratio d/h_{Tx}). As expected from the results in Section III-B2, when $d \gg h_{Tx}$, SDF's beam is unaffected by the presence of the ground plane. However, one notices additionally that even when d decreases with respect to h_{Tx}, only very slight variations in the BER profile appear and thus that SDF is still applicable in these scenarios.

This is easily explained by recalculating $\Delta\tau_l^{MPC}$ for a receiver in close proximity of the base station. In the specific scenario that is simulated, i.e. $N = 2$, the LOS path length to a receiver in broadside is equal for both antennas, regardless of its distance to the transmitter. As a result, using the exact expression (11c), the path lengths of the ground reflected rays are equal as well and $\Delta\tau_l^{MPC}$ is zero in broadside, thus not distorting the symbols. $\Delta\tau_l^{MPC}$ will increase and vary from $\Delta\tau_l^{LOS}$ when receivers move away from broadside and hence cause additional undesired symbol distortion. However this is of no importance since the symbol distortion and hence the BER are expected to be high in these regions. Note that, as long as the paraxial approximation is satisfied, this is true regardless of the number of antennas in the array.

IV. Conclusion and Perspectives

By performing Spatial Data Focusing (SDF) instead of the traditional power focusing, it was proven that considerably narrower beams, evaluated as angular regions around a transmitter where the BER is below a threshold, can be created. As a consequence, accurate broadcasting of data to specific spatial locations is possible, making SDF an attractive technique for use in geocasting applications. Since focusing is performed by exploiting the path length differences between the channels of an array, that are inherently present for receivers not in the broadside direction of this array, SDF does not require complex transmitter infrastructures and can be implemented using relatively simple modulations techniques. Furthermore, it was shown that, when using linear arrays in an over-the-ground propagation environment, the performance of SDF is identical to pure LOS environments, without the need for additional techniques to increase robustness.

References

[1] K. Seada and A. Helmy, "Efficient geocasting with perfect delivery in wireless networks," *2004 IEEE Wireless Communications and Networking Conference (IEEE Cat. No.04TH8733)*, Atlanta, GA, USA, 2004, pp. 2551–2556 Vol.4.

[2] Y.-B. Ko and N. H. Vaidya, "Geocasting in mobile ad hoc networks: location-based multicast algorithms," *Proceedings WMCSA'99. Second IEEE Workshop on Mobile Computing Systems and Applications*, New Orleans, LA, USA, 1999, pp. 101–110.

[3] C.A. Balanis, "Arrays: Linear, Planar, and Circular," in *Antenna Theory, analysis and design*, 3rd ed. Hoboken, New Jersey, USA: John Wiley & Sons, Inc., 2005, ch. 6, sec. 6.1–6.8, pp. 283–344.

[4] A. Babakhani, D. B. Rutledge and A. Hajimiri, "Transmitter Architectures Based on Near-Field Direct Antenna Modulation," in *IEEE Journal of Solid-State Circuits*, vol. 43, no. 12, pp. 2674–2692, Dec. 2008.

[5] M. P. Daly and J. T. Bernhard, "Beamsteering in Pattern Reconfigurable Arrays Using Directional Modulation," in *IEEE Transactions on Antennas and Propagation*, vol. 58, no. 7, pp. 2259–2265, July 2010.

[6] M. P. Daly and J. T. Bernhard, "Directional Modulation Technique for Phased Arrays," in *IEEE Transactions on Antennas and Propagation*, vol. 57, no. 9, pp. 2633–2640, Sept. 2009.

[7] M. P. Daly, E. L. Daly and J. T. Bernhard, "Demonstration of Directional Modulation Using a Phased Array," in *IEEE Transactions on Antennas and Propagation*, vol. 58, no. 5, pp. 1545–1550, May 2010.

[8] Y. Ding and V. Fusco, "Orthogonal Vector Approach for Synthesis of Multi-Beam Directional Modulation Transmitters," in *IEEE Antennas and Wireless Propagation Letters*, vol. 14, pp. 1330–1333, 2015.

[9] S. Mufti, J. Parrón and A. Tennant, "Hardware implementation of directional modulation system with a 2 element antenna array," *2017 11th European Conference on Antennas and Propagation (EUCAP)*, Paris, 2017, pp. 3239–3242.

[10] J. Sarrazin, M. Odhiambo, S. Golstein, P. De Doncker and F. Horlin, "Spatial Data Focusing: An Alternative to Beamforming for Geocasting Scenarios," *2018 USNC-URSI Radio Science Meeting (Joint with AP-S Symposium)*, Boston, MA, 2018, pp. 139–140.